AGU PUBLICATIONS

Geophysical Research Letters

RESEARCH LETTER
10.1002/2015GL063796

Key Points:
- The water column in Ryder Bay is a net, annual sink of atmospheric CO_2
- Seasonal sea ice increases the strength of the ocean CO_2 sink in Ryder Bay
- Large uncertainty remains regarding the effect of sea ice on gas exchange

Supporting Information:
- Text S1

Correspondence to:
O. J. Legge,
o.legge@uea.ac.uk

Citation:
Legge, O. J., D. C. E.Bakker, M. T. Johnson, M. P. Meredith, H. J. Venables, P. J. Brown, and G. A. Lee (2015), The seasonal cycle of ocean-atmosphere CO_2 flux in Ryder Bay, west Antarctic Peninsula, *Geophys. Res. Lett.*, *42*, 2934–2942, doi:10.1002/2015GL063796.

Received 9 MAR 2015
Accepted 19 MAR 2015
Accepted article online 25 MAR 2015
Published online 28 APR 2015

The seasonal cycle of ocean-atmosphere CO_2 flux in Ryder Bay, west Antarctic Peninsula

Oliver J. Legge[1,2], Dorothee C. E. Bakker[1], Martin T. Johnson[1,3], Michael P. Meredith[2], Hugh J. Venables[2], Peter J. Brown[4], and Gareth A. Lee[1]

[1]Centre for Ocean and Atmospheric Sciences, School of Environmental Sciences, University of East Anglia, Norwich, UK, [2]British Antarctic Survey, Cambridge, UK, [3]Centre for Environment Fisheries and Aquaculture Science, Lowestoft, UK, [4]National Oceanography Centre, University of Southampton, Southampton, UK

Abstract Approximately 15 million km^2 of the Southern Ocean is seasonally ice covered, yet the processes affecting carbon cycling and gas exchange in this climatically important region remain inadequately understood. Here, 3 years of dissolved inorganic carbon (DIC) measurements and carbon dioxide (CO_2) fluxes from Ryder Bay on the west Antarctic Peninsula (WAP) are presented. During spring and summer, primary production in the surface ocean promotes atmospheric CO_2 uptake. In winter, higher DIC, caused by net heterotrophy and vertical mixing with Circumpolar Deep Water, results in outgassing of CO_2 from the ocean. Ryder Bay is found to be a net sink of atmospheric CO_2 of 0.59–0.94 mol Cm^{-2} yr^{-1} (average of 3 years). Seasonal sea ice cover increases the net annual CO_2 uptake, but its effect on gas exchange remains poorly constrained. A reduction in sea ice on the WAP shelf may reduce the strength of the oceanic CO_2 sink in this region.

1. Introduction

The Southern Ocean south of 44°S is responsible for approximately 25–30% of the global ocean uptake of anthropogenic carbon [*Fletcher et al.*, 2006; *Lenton et al.*, 2013], but accurately quantifying this sink and understanding the processes behind it remains challenging. The net ocean-atmosphere CO_2 flux of the high-latitude, seasonally ice-covered Southern Ocean is especially difficult to quantify due to a scarcity in observational data, particularly during the ice-covered winter months [*Bakker et al.*, 2014]. Not only does ice cover hinder data collection and therefore limit the scope of observational flux estimates, but it also adds complexity to the carbon cycle through its effect on gas exchange, vertical stability, and biological production.

Estimates of CO_2 uptake by the high-latitude Southern Ocean vary between models, inversions, and observations. Most recent estimates characterize the high-latitude Southern Ocean as a small sink or a small source of CO_2 to the atmosphere [*Gruber et al.*, 2009; *Takahashi et al.*, 2009; *Lenton et al.*, 2013]; however, they are largely based on the open ocean and do not account for the variability and importance of the coastal ocean which may be a strong sink of CO_2 [*Arrigo et al.*, 2008]. Furthermore, many ocean biogeochemical models fail to capture the magnitude of the seasonal cycle at high latitudes, the main mode of variability in this region [*Lenton et al.*, 2013]. This inability to reconcile modeled and observed CO_2 fluxes highlights our poor understanding of the high-latitude carbon cycle and limits confidence in our ability to predict future changes to Southern Ocean CO_2 uptake.

Recent work suggests that the Southern Ocean carbon sink may be weakening, and this has been attributed to increased upwelling of dissolved inorganic carbon (DIC) caused by increased Southern Ocean winds associated with a more positive Southern Annular Mode (SAM) [*Lenton and Matear*, 2007; *Le Quéré et al.*, 2007; *Lovenduski et al.*, 2008]—a climatic change that is known to include an anthropogenic component [*Thompson and Solomon*, 2002]. However, due to a lack of observational data in this region, our mechanistic understanding of the variability in the ocean-atmosphere flux of CO_2 remains weak. A better understanding of the processes driving seasonal and interannual variablity in carbon flux is required to strengthen our predictions of future carbon uptake by the Southern Ocean. This is true especially for the productive coastal waters, which are the focus of this paper.

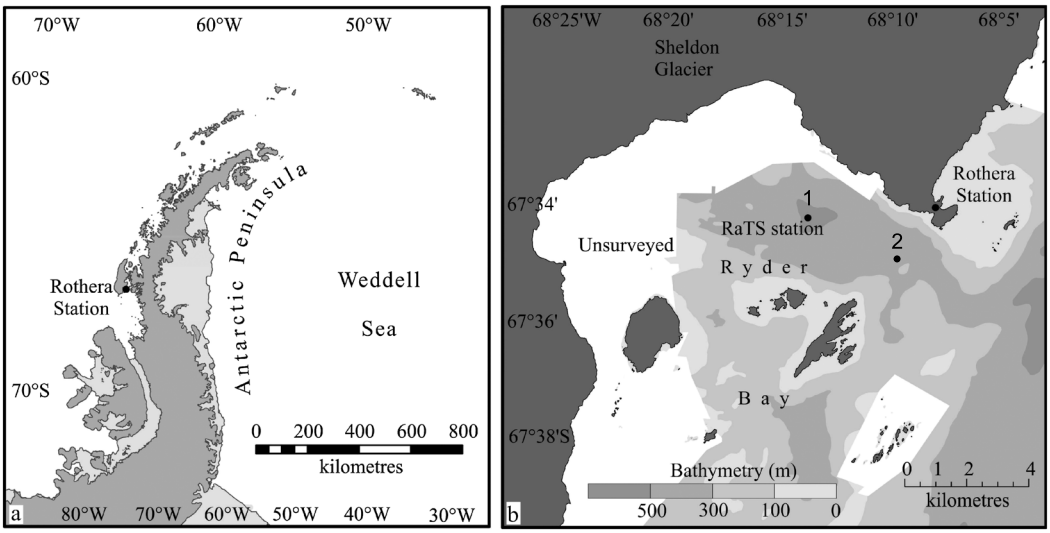

Figure 1. (a) Location of Rothera on Adelaide Island at the west Antarctic Peninsula. (b) Location of RaTS sites 1 and 2 in Ryder Bay. Modified from *Venables et al.* [2013].

2. Methods

2.1. Sampling and Analyses

Discrete samples for dissolved inorganic carbon (DIC) and total alkalinity (TA) were collected from 15m depth at the Rothera Time Series site (RaTS), located in Ryder Bay, about 4km offshore on the west Antarctic Peninsula (Figure 1). Sampling was undertaken from a rigid inflatable boat or through a hole in the ice approximately weekly in summer and biweekly in winter, weather and ice permitting. If partial ice cover prevented access to the main RaTS site, then a secondary site was used (Figure 1). Collection of inorganic carbon samples began in December 2010 and continued until February 2014. Samples were collected in 250 ml or 500 ml borosilicate glass bottles, spiked with mercuric chloride and sealed with greased stoppers. They were transported back to the University of East Anglia, UK, at the end of each field season for analysis. DIC was measured by coulometry [*Johnson et al.*, 1985] following standard operating procedure (SOP) 2 of *Dickson et al.* [2007], and TA was measured by potentiometric titration [*Mintrop et al.*, 2000] following SOP 3b of *Dickson et al.* [2007]. DIC and TA were measured using two VINDTAs (versatile instrument for the determination of titration alkalinity, version 3C, Marianda, Germany). Instruments were calibrated using certified reference materials from the Scripps Institution of Oceanography. Sea ice type and fraction of ice cover were visually estimated by marine assistants at Rothera. While these sea ice estimates are inherently somewhat subjective, the Rothera data have been found to agree well with wider-scale satellite estimates [*Wallace*, 2007]. Temperature, salinity, and pressure were measured during full depth (500m at site 1) conductivity, temperature, depth (CTD) casts [*Venables et al.*, 2013].

2.2. Ocean-Atmosphere CO_2 Flux

The ocean-atmosphere flux of CO_2 was calculated for each day during the study period using equation (1). A negative value signifies an uptake from the atmosphere by the ocean.

$$CO_2\text{flux} = s \cdot \Delta fCO_2 \cdot k \quad (1)$$

where s is the solubility of CO_2 at in situ temperature and salinity, calculated using the equation of *Weiss* [1974], ΔfCO_2 is the difference in the fugacity of CO_2 between seawater and the air, and k is the gas transfer velocity. Water fCO_2 was calculated from DIC, TA, silicate, and phosphate measurements using the CO2SYS program [*Van Heuven et al.*, 2011]. Total alkalinity data are presented in the supporting information. Seawater temperature and salinity, seawater fCO_2, and open water fraction were linearly interpolated into daily vectors. Atmospheric fCO_2 was calculated from the dry mole fraction of CO_2 (xCO_2) using the coefficients of *Weiss* [1974], and water vapor pressure was calculated following *Weiss and Price* [1980]. Atmospheric xCO_2 data are from weekly flask samples from Palmer Station, approximately 400km northeast of Rothera [*Dlugokencky et al.*, 2014]. These discrete flask data were interpolated and smoothed using a

weighted linear least squares method. Daily averaged wind speed and sea level pressure were measured at Rothera. Wind speed has been corrected from the measurement height of 42 m to 10 m above sea level following *Fairall et al.* [2011].

2.3. Ice Cover and Gas Transfer Velocity

Gas transfer velocity (k) and its relationship with ice cover were calculated using two separate methods. First, k was calculated from wind speed using the parameterization of *Wanninkhof et al.* [2013]. As in previous studies, the gas transfer velocity was scaled linearly with sea ice cover by multiplying k by the fraction of open water. Even at 100% ice cover, there is likely to be some gas exchange with the atmosphere due to leads, fractures, and brine channels [*Semiletov et al.*, 2004; *Loose and Schlosser*, 2011], so, consistent with other studies [*Bates et al.*, 2006; *Mucci et al.*, 2010; *Roden et al.*, 2013], we have set the minimum open water fraction to 0.01. A scenario with no ice is also considered in which k is not modified by ice cover and also a scenario in which brash and grease ice do not affect k. The second method for calculating gas transfer velocity is a recently published parameter model for gas exchange in the sea ice zone [*Loose et al.*, 2014]. This model relates k to wind speed through mean squared wave slope and also includes shear-driven and convection-driven turbulence. The k derived from both methods was corrected to the Schmidt number following *Wanninkhof* [1992]. Full details of gas flux calculations are given in the supporting information.

2.4. Uncertainties

Uncertainties were calculated from the measurement uncertainty of DIC, TA, silicate, phosphate, and atmospheric CO_2; the uncertainty of the carbonate system dissociation constants [*Millero*, 2007]; and the uncertainty of the parameterization of the gas transfer velocity [*Wanninkhof*, 2014]. The propagation of uncertainties using a Monte Carlo approach is described in Appendix A.

3. Results and Discussion

3.1. Seasonal and Interannual Variability

The 3 years of DIC data presented here (Figure 2) display a clear, highly assymetric, seasonal cycle with an amplitude of ~200 μmol kg^{-1}. DIC decreases sharply during December/January due to the rapid increase of biological production, and summer months are characterized by low and variable DIC values. There is a gradual increase from around April to maximum DIC concentrations of ~2200 μmol kg^{-1} in September. This increase during autumn and winter is caused by net heterotrophy and mixing with relatively old, carbon-rich Circumpolar Deep Water (CDW) as the mixed layer deepens. The rapid spring DIC drawdown is preceded by a more gradual decrease corresponding to reduced sea ice cover (Figure 2), an increase in photosynthetically active radiation, and a shoaling and warming mixed layer. The gradual decrease prior to the main spring bloom is therefore likely to be caused by the onset of algal production in the water column and ice but may also be influenced by ikaite dissolution during ice melt (see section 3.2).

Due to the pronounced seasonal cycle in DIC, the ΔfCO_2 changes sign between winter and summer (Figure 2), making the water column a potential source of CO_2 to the atmosphere during winter and a potential sink during summer. This gradient determines the direction of the CO_2 flux, but its magnitude is strongly influenced by wind speed and ice cover. The daily ocean-atmosphere CO_2 flux, as calculated with a linear scaling between k and ice cover (Figure 3), ranges from approximately −15 mol Cm^{-2} yr^{-1} in summer (into the ocean) to approximately 10 mol Cm^{-2} yr^{-1} in winter (out of the ocean). In all 3 years sampled, the summer uptake of CO_2 by the ocean is greater than the winter outgassing, making the water column in Ryder Bay a net sink of atmospheric CO_2 over an annual cycle. Summing the daily fluxes gives the cumulative ocean-atmosphere CO_2 flux (Figure 3), clearly showing a net ocean sink from all estimates. The mean net annual CO_2 uptake by the ocean from 1 January 2011 to 31 December 2013 was 0.59 mol Cm^{-2} yr^{-1} as calculated using the linear scaling of k with ice cover (solid blue line, Figure 3) with net annual uptake ranging from 0.22 mol Cm^{-2} yr^{-1} in 2013 to 1.03 mol Cm^{-2} yr^{-1} in 2011. When calculated using the sea ice gas exchange model (solid red line, Figure 3), the mean net annual ocean uptake was 0.94 mol Cm^{-2} yr^{-1} ranging from 0.47 mol Cm^{-2} yr^{-1} in 2013 to 1.50 mol Cm^{-2} yr^{-1} in 2011. Our estimates of net annual ocean carbon uptake using a linear k scaling are similar to the estimate of *Roden et al.* [2013], who calculated a net ocean uptake in Prydz Bay, East Antarctica of 0.54 ± 0.11 mol Cm^{-2} yr^{-1}, also using a linear scaling of k with ice cover. Our estimates are somewhat lower than the net annual CO_2 uptake of the Ross Sea, estimated using a biogeochemical model as 1.7–4.2 mol Cm^{-2} yr^{-1} [*Arrigo et al.*, 2008].

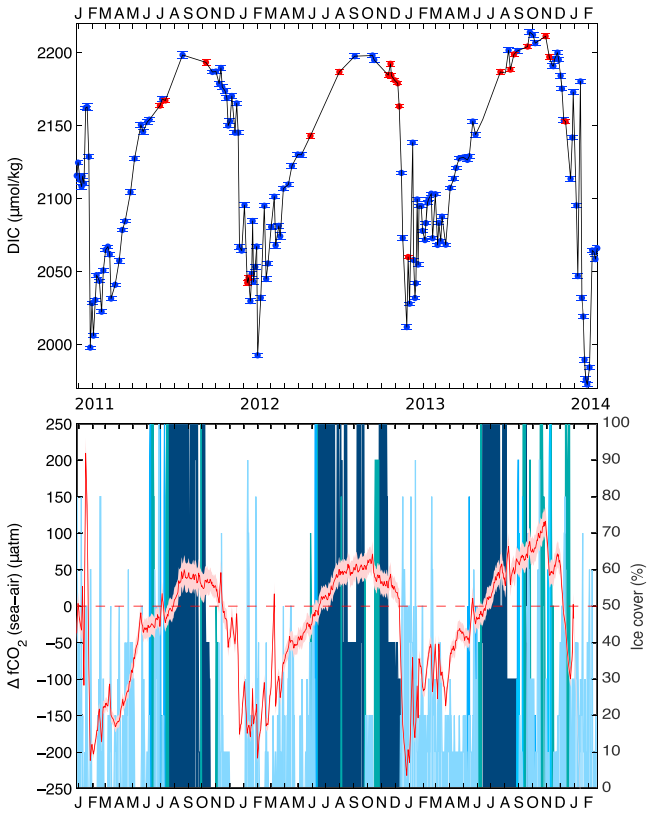

Figure 2. (top) The seasonal cycle of dissolved inorganic carbon from December 2010 until February 2014 at 15m depth at RaTS. Blue points indicate data from site 1, red from site 2. Error bars are uncertainty (2SD) based on measurement precision. (bottom) The red line represents the seasonal cycle of ΔfCO_2 with the shaded region representing approximate 95% confidence from uncertainty analysis. The red dashed line shows $\Delta fCO_2 = 0$, i.e., ocean CO_2 concentration is at equilibrium with the atmosphere. Blue bars show percentage ice cover. Bar color denotes ice type with dark blue representing fast ice, turquoise representing pack ice, and light blue representing brash ice.

There is significant interannual variability in the ocean-atmosphere flux of CO_2, especially in the amount of winter outgassing (Figure 3). Atmospheric CO_2 increases by roughly 2.3 ppm/yr from ~387 ppm in January 2011 to ~394 ppm in January 2014, with a seasonal amplitude of ~3 ppm. Despite this increase in atmospheric CO_2 during the study period, the ocean to atmosphere CO_2 flux increases through each successive winter in the three observed years, and we hypothesize that this interannual variability is caused by two main drivers. First, higher water fCO_2 in winter increases the concentration gradient of CO_2 between the ocean and the atmosphere (Figure 2), making the ocean a stronger potential source of CO_2 to the atmosphere. We suggest that the increase in fCO_2 and DIC in surface water in winter is caused by increased mixing of CDW into the surface layer, and this theory is supported by a slight increase in winter salinity from 2011 to 2013. Reduced ice cover in Ryder Bay during winter allows enhanced mixing due to the exposed water surface, and this can result in reduced stratification in the following spring [*Venables and Meredith*, 2014]. A decrease in ice cover could therefore affect ocean-atmosphere CO_2 fluxes by increasing the mixing of CDW into the surface and increasing surface water fCO_2 and DIC.

Second, a reduction in ice cover during winter, when ΔfCO_2 is positive, allows more gas exchange across the air-water interface. The three consecutive winters shown here exhibit increasing ΔfCO_2 and a longer period during which ΔfCO_2 is positive, while ice cover is below 50%. These factors combined result in increased outgassing of CO_2 to the atmosphere and a reduced net CO_2 sink over the seasonal cycle. When the effect of ice cover on k is ignored, the water column is still found to be a net sink of atmospheric CO_2 (dashed lines, Figure 3), although the strength of this sink is reduced compared with the equivalent calculations including ice cover (solid blue and red lines, Figure 3). The role of winter sea ice cover in reducing CO_2 flux from the ocean to the atmosphere is consistent with previous observations [*Gibson and Trull*, 1999; *Sweeney*, 2003;

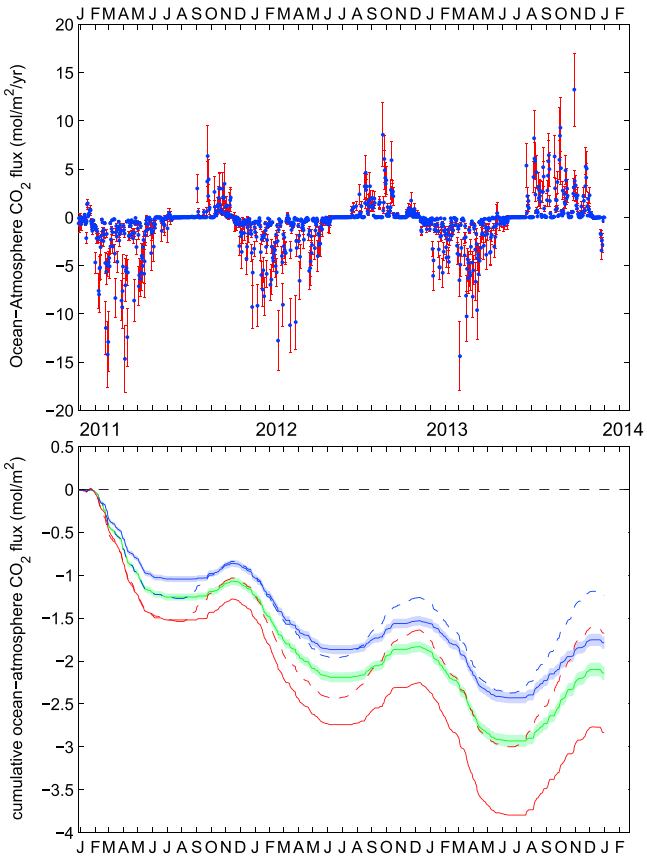

Figure 3. (top) Ocean-atmosphere CO_2 flux at RaTS, calculated using a linear scaling between *k* and all ice types (corresponds to solid blue line in Figure 3, bottom). Error bars represent approximate 95% confidence. (bottom) Cumulative ocean-atmosphere flux of CO_2 at RaTS. Blue line represents flux calculated following *Wanninkhof et al.* [2013] with a linear scaling of *k* to sea ice cover. Green line also represents flux calculated following *Wanninkhof et al.* [2013] but excluding brash ice. Shaded regions represent approximate 95% confidence, calculated as the square root of the cumulative sum of the squares. Blue dashed line represents flux calculated following *Wanninkhof et al.* [2013] assuming no ice cover. Red line represents flux calculated using the model of *Loose et al.* [2014], including all ice types. Red dashed line represents flux calculated with the model of *Loose et al.* [2014] but assuming no ice cover.

Bakker et al., 2008] and supports the hypothesis that increased Antarctic sea ice cover during glacial periods could have lowered atmospheric CO_2 by reducing deep water ventilation [*Stephens and Keeling*, 2000].

3.2. Unresolved Complexity

Quantification of the gas transfer velocity in ice-covered or partially ice-covered waters is challenging, particularly as different ice types are likely to affect gas fluxes in different ways, and this heterogeneity is not well understood. To investigate the sensitivity of our flux estimates to different ice types, ocean-atmosphere CO_2 flux was also calculated with brash ice ignored (green line, Figure 3). This scenario results in a stronger annual ocean uptake of CO_2 than when *k* is affected by all ice types (solid blue line) because brash ice predominates in summer, when the ΔfCO_2 is negative, so its removal allows more CO_2 flux into the water. The parameter model of *Loose et al.* [2014] (red line, Figure 3) gives higher *k* values and therefore a larger net annual sink than the scenario using a linear scaling of *k* with ice cover. This is partly caused by the way in which these two methods calculate *k* from wind speed. The contribution of this factor can be seen as the difference between the red and blue dashed lines which do not include ice effects. Another reason for the discrepancy between the linear scaling and the parameter model is the inclusion in the model of shear-driven and convection-driven turbulence which can increase the gas transfer velocity by 40% [*Loose et al.*, 2014]. It is important to note that the uncertainty caused by the handling of ice cover and ice type in gas flux estimates dwarfs that caused by uncertainty in the carbonate parameters and the gas transfer

velocity (shading on blue and green lines, Figure 3). More observational data, from both laboratory ice tank experiments and field studies, are needed to increase our confidence in calculating ocean-atmosphere gas flux in seasonally ice-covered waters.

As carbon samples were collected from 15 m depth, the seawater fCO_2 used for flux calculations may not accurately represent surface concentrations when the mixed layer shoals to above this depth in summer. Due to biological activity in the surface mixed layer, it is likely that our water fCO_2 is overestimated between approximately December and March, giving an underestimate of the difference between the concentration of CO_2 in the atmosphere and the sea water. The net annual ocean CO_2 uptake presented here is therefore likely to be an underestimate. Mixed layer depth data are presented in the supporting information.

Sea ice does not simply act as a cap to ocean-atmosphere gas exchange; sea ice-atmosphere CO_2 exchange has been observed in both the Arctic and Antarctic [*Gosink et al.*, 1976; *Semiletov et al.*, 2004; *Delille*, 2006; *Zemmelink et al.*, 2006; *Miller et al.*, 2011; *Nomura et al.*, 2013]. The estimates of CO_2 flux presented here do not account for these ice-atmosphere interactions and so may overestimate or underestimate the net annual sink of the water column. Although sea ice has been demonstrated to act as both a source and a sink of CO_2 over the seasonal cycle [*Delille et al.*, 2014], we have applied the maximum flux of CO_2 from Antarctic sea ice to the atmosphere of 1.9 mmol m^{-2} d^{-1} observed by *Delille et al.* [2014] in order to obtain a first-order estimate of the maximum possible reduction in CO_2 sink strength caused by ice cover. Multiplying the percentage cover of fast or pack ice in Ryder Bay during the study period by this value results in a weakening of the net annual sink of atmospheric CO_2 of approximately 0.2 mol m^{-2} yr^{-1}.

As well as modulating gas exchange via physical processes, sea ice also affects CO_2 flux through its effect on carbonate chemistry. The precipitation of the hydrated calcium carbonate mineral ikaite ($CaCO_3 \cdot 6H_2O$) in sea ice increases CO_2 in brine, and its dissolution on ice melt reduces CO_2 of the seawater [*Rysgaard et al.*, 2011]. Although no carbon measurements in sea ice were made here, ikaite has been observed in Antarctic sea ice [*Dieckmann et al.*, 2008] and has been found to significantly increase brine pCO_2 during precipitation and decrease brine pCO_2 on dissolution [*Papadimitriou et al.*, 2004; *Delille et al.*, 2007; *Geilfus et al.*, 2012]. *Rysgaard et al.* [2012] found the dissolution of ikaite during sea ice melt to correspond to an air-sea CO_2 uptake of ~3.9 mol Cm^{-2} yr^{-1}, given a reduction in ice thickness of 0.2 m/week. This process is of a significant magnitude compared to the ocean-atmosphere CO_2 fluxes presented here (Figure 3). It is likely that some of the increase in water pCO_2 observed during winter in Ryder Bay is caused by the release of high CO_2 brine from sea ice and, similarly, that some of the fCO_2 decrease observed in spring is caused by ikaite dissolution. However, the quantification of the impact of ice formation/melt on carbonate chemistry in Ryder Bay is complicated by the fact that an observed change in ice cover is not directly related to ice formation/melt as much of the brash and pack ice may be blown in/out of the bay rather than forming/melting in situ [*Meredith et al.*, 2010]. Biological production by ice algae was also not quantified quantified here and it almost certainly contributes to reducing DIC and fCO_2 in the surface layer, thereby affecting the ocean-atmosphere CO_2 flux in spring.

3.3. Future Implications

The mechanistic understanding of observed variability in the ocean CO_2 uptake that we have developed has significant implications for how we can expect the carbon sink in this region to behave in the future. The west Antarctic Peninsula has been one of the most rapidly warming regions in the world over the last 50 years [*Vaughan et al.*, 2003; *Meredith and King*, 2005] with an associated rapid decrease in sea ice cover [*Stammerjohn et al.*, 2008; *Li et al.*, 2014]. On a larger scale, and contemporaneous with this, there has been a strengthening of zonal winds south of 45°S, which is projected to increase in future [*Le Quéré et al.*, 2007], and modeling studies suggest that this will increase the upwelling of carbon-rich deep water in the Southern Ocean, slowing the increase in the carbon sink expected with rising atmospheric CO_2 levels [*Lenton and Matear*, 2007; *Lovenduski et al.*, 2008]. Decadal changes in the properties and production of dense water around Antarctica have also been observed [*Meredith et al.*, 2014; *Purkey and Johnson*, 2012; *Lavergne et al.*, 2014], emphasizing further the potential sensitivity of the Southern Ocean carbon sink to climatic change. The observations presented here support the theory that reduced winter ice cover and increased surface DIC concentrations in future will reduce the rate at which the region takes up atmospheric CO_2. Furthermore, a reduction in the spring phytoplankton bloom in Ryder Bay following winters with reduced sea ice

Table A1. Uncertainties Associated With Measured Parameters, Carbonate System Constants, and the Gas Transfer Velocity

Parameter	Uncertainty (1 SD)	Unit	Source
DIC	2.2	μmol kg^{-1}	Long-term precision of CRM analyses
TA	1.3	μmol kg^{-1}	Long-term precision of CRM analyses
Silicate	2.6	%	Precision quoted by analyst
Phosphate	2.7	%	Precision quoted by analyst
pK1	0.0055	-	Constant from *Goyet and Poisson* [1989]; uncertainty from *Millero* [2007]
pK2	0.01	-	Constant from *Goyet and Poisson* [1989]; uncertainty from *Millero* [2007]
Atmospheric CO_2	0.23	ppm	RMSE of the smoothed, interpolated data versus the measured values at Palmer station.
Gas transfer velocity	20	%	*Wanninkhof* [2014]

cover has been found [*Venables et al.*, 2013], and it has been suggested that a continued reduction in WAP sea ice cover is likely to lead to reduced phytoplankton blooms in the region. A reduction in winter sea ice would therefore not only increase winter outgassing but would also reduce summer uptake of CO_2 by the ocean, further reducing the net annual CO_2 sink.

Appendix A: Uncertainties

Uncertainties were calculated using a Monte Carlo approach to ensure that all nonlinearities in the carbon system calculations were accounted for in error propagation. This is hard to achieve using formal error propagation. The propagation of uncertainties was divided into two steps. First, the uncertainty on water fCO_2 for each measurement of DIC and TA was calculated as follows: 10^5 parameter value sets were created including the parameters DIC, TA, silicate, phosphate, pK1, and pK2. For each parameter, values were determined by random sampling from a distribution based on the measured value (or calculated value in the case of carbonate system constants) as the population mean with a standard deviation based on the measurement or parameter uncertainty (see Table A1). The CO2SYS program was run on each set of parameter values to determine a probability density function (pdf) for fCO_2, twice the standard deviation of which was taken as a measure of that data point's uncertainty. The errors on measured values and carbonate system constants used in the uncertainty analysis (see Table A1) were assumed to be normally distributed. One standard deviation was used to define the characteristics of the distribution of each of the input parameters in the uncertainty analysis. Two standard deviations (approximately 95% confidence) is quoted when referring to calculated uncertainties.

The second step was the calculation of uncertainty on the daily calculated ocean-atmosphere flux. Following interpolation of all input parameters on a daily basis, the uncertainty on each daily calculated flux was calculated as follows: 10^5 parameter value sets were created for water fCO_2, air fCO_2, and k as described above. The uncertainty on water fCO_2 was taken from the previous step, the uncertainty on air fCO_2 is described in Table A1, and the uncertainty on k was taken as 20% [*Wanninkhof*, 2014] and given a uniform distribution. The ocean-atmosphere flux was calculated for each set of values as above, and twice the standard deviation of the resulting pdf was taken as a measure of the uncertainty of that day's flux. The uncertainty on the cumulative flux was calculated as the square root of the sum of the squares of the uncertainties up to and including each point which assumes randomly distributed rather than systematic uncertainty. Uncertainties were only quantified for the fluxes calculated following *Wanninkhof et al.* [2013] with a linear scaling of ice cover and k. The uncertainty on the fluxes calculated following *Loose et al.* [2014] was not quantified as the uncertainties in this new model are not well understood.

Acknowledgments
This work is part of PhD research funded by the Natural Environment Research Council(NERC) (NE/L50158X/1). This work was also supported by BAS Polar Oceans funding from NERC and the UK Ocean Acidification Research Programme (NE/H017046/1). We would like to thank the BAS marine assistants Sabrina Heiser, Mairi Fenton, and Simon Reeves for sample collection and UEA technicians Stephen Humphrey and Matt Von Tersch for assistance with DIC and TA analyses. We would also like to thank Brice Loose whose constructive comments have improved the manuscript. Data availability: Marine data from RaTS are lodged with the British Oceanographic Data Centre and are available from them upon request (contact: enquiries@bodc.ac.uk). Atmospheric data from Rothera are available online at www.antarctica.ac.uk/met/metlog/. Atmospheric CO_2 data are available online from NOAA at ftp://aftp.cmdl.noaa.gov/data/trace_gases/co2/flask/surface/co2_psa_surface-flask_1_ccgg_event.txt.

The Editor thanks an anonymous reviewer for his/her assistance in evaluating this paper.

References

Arrigo, K. R., G. van Dijken, and M. Long (2008), Coastal Southern Ocean: A strong anthropogenic CO_2 sink, *Geophys. Res. Lett.*, *35*, L21602, doi:10.1029/2008GL035624.

Bakker, D. C. E., M. Hoppema, M. Schroder, W. Geibert, and H. J. W. de Baar (2008), A rapid transition from ice covered CO_2 rich waters to a biologically mediated CO_2 sink in the eastern Weddell Gyre, *Biogeosciences*, *5*, 1373–1386.

Bakker, D. C. E., et al. (2014), An update to the Surface Ocean CO_2 Atlas (SOCAT version 2), *Earth Syst. Sci. Data*, *6*(1), 69–90, doi:10.5194/essd-6-69-2014.

Bates, N. R., S. B. Moran, D. a. Hansell, and J. T. Mathis (2006), An increasing CO_2 sink in the Arctic Ocean due to sea-ice loss, *Geophys. Res. Lett.*, *33*, L23609, doi:10.1029/2006GL027028.

Delille, B. (2006), Inorganic carbon dynamics and air-ice-sea CO_2 fluxes in the open and coastal waters of the Southern Ocean, PhD thesis, Univ. of Liege, Belgium.

Delille, B., B. Jourdain, A. V. Borges, and D. Delille (2007), Biogas (CO_2, O_2, dimethylsulfide) dynamics in spring Antarctic fast ice, *Limnol. Oceanogr.*, *52*(4), 1367–1379.

Delille, B., et al. (2014), Southern Ocean CO_2 sink: The contribution of the sea ice, *J. Geophys. Res. Oceans*, *119*, 6340–6355, doi:10.1002/2014JC009941.

Dickson, A. G., C. Sabine, and J. R. Christian (2007), *Guide to Best Practices for Ocean CO_2 Measurements, PICES Spec. Publ.*, vol. 3, 191 pp., North Pacific Mar. Sci. Organ., Sidney, Canada.

Dieckmann, G. S., G. Nehrke, S. Papadimitriou, J. Göttlicher, R. Steininger, H. Kennedy, D. Wolf-Gladrow, and D. N. Thomas (2008), Calcium carbonate as ikaite crystals in Antarctic sea ice, *Geophys. Res. Lett.*, *35*, L08501, doi:10.1029/2008GL033540.

Dlugokencky, E., P. Lang, K. Masarie, A. M. Crotwell, and M. J. Crotwell (2014), Atmospheric Carbon Dioxide Dry Air Mole Fractions from the NOAA ESRL Carbon Cycle Cooperative Global Air Sampling Network, 1968-2013, Version: 2014-06-27. [Available at ftp://aftp.cmdl.noaa.gov/data/trace_gases/co2/flask/surface/.]

Fairall, C. W., M. Yang, L. Bariteau, J. B. Edson, D. Helmig, W. McGillis, S. Pezoa, J. E. Hare, B. Huebert, and B. Blomquist (2011), Implementation of the coupled ocean-atmosphere response experiment flux algorithm with CO_2, dimethyl sulfide, and O_3, *J. Geophys. Res.*, *116*, C00F09, doi:10.1029/2010JC006884.

Fletcher, S. E. M., et al. (2006), Inverse estimates of anthropogenic CO_2 uptake, transport, and storage by the ocean, *Global Biogeochem. Cycles*, *20*, GB2002, doi:10.1029/2005GB002530.

Geilfus, N.-X., G. Carnat, T. Papakyriakou, J.-L. Tison, B. Else, H. Thomas, E. Shadwick, and B. Delille (2012), Dynamics of pCO_2 and related air-ice CO_2 fluxes in the Arctic coastal zone (Amundsen Gulf, Beaufort Sea), *J. Geophys. Res.*, *117*, C00G10, doi:10.1029/2011JC007118.

Gibson, J. A. E., and T. W. Trull (1999), Annual cycle of fCO_2 under sea-ice and in open water in Prydz Bay, East Antarctica, *Mar. Biol.*, *66*, 187–200.

Gosink, T., J. Pearson, and J. Kelley (1976), Gas movement through sea ice, *Nature*, *263*, 41–42.

Goyet, C., and A. Poisson (1989), New determination of carbonic acid dissociation constants in seawater as a function of temperature and salinity, *Deep Sea Res., Part A*, *36*(11), 1635–1654.

Gruber, N., et al. (2009), Oceanic sources, sinks, and transport of atmospheric CO_2, *Global Biogeochem. Cycles*, *23*, GB1005, doi:10.1029/2008GB003349.

Johnson, K., A. King, and J. Sieburth (1985), Coulometric TCO_2 analyses for marine studies; and introduction, *Mar. Chem.*, *16*, 61–82.

Lavergne, C. D., J. B. Palter, E. D. Galbraith, R. Bernardello, and I. Marinov (2014), Cessation of deep convection in the open Southern Ocean under anthropogenic climate change, *Nat. Clim. Change*, *4*, 278–282, doi:10.1038/NCLIMATE2132.

Le Quéré, C., et al. (2007), Saturation of the Southern Ocean CO_2 sink due to recent climate change, *Science*, *316*, 1735–1737.

Lenton, A., and R. J. Matear (2007), Role of the Southern Annular Mode (SAM) in Southern Ocean CO_2 uptake, *Global Biogeochem. Cycles*, *21*, GB2016, doi:10.1029/2006GB002714.

Lenton, A., et al. (2013), Sea-air CO_2 fluxes in the Southern Ocean for the period 1990–2009, *Biogeosci. Discuss.*, *10*(1), 285–333, doi:10.5194/bgd-10-285-2013.

Li, X., D. M. Holland, E. P. Gerber, and C. Yoo (2014), Impacts of the north and tropical Atlantic Ocean on the Antarctic Peninsula and sea ice, *Nature*, *505*(7484), 538–542, doi:10.1038/nature12945.

Loose, B., and P. Schlosser (2011), Sea ice and its effect on CO_2 flux between the atmosphere and the Southern Ocean interior, *J. Geophys. Res.*, *116*, C11019, doi:10.1029/2010JC006509.

Loose, B., W. R. McGillis, D. Perovich, C. J. Zappa, and P. Schlosser (2014), A parameter model of gas exchange for the seasonal sea ice zone, *Ocean Sci.*, *10*, 1–12, doi:10.5194/os-10-1-2014.

Lovenduski, N. S., N. Gruber, and S. C. Doney (2008), Toward a mechanistic understanding of the decadal trends in the Southern Ocean carbon sink, *Global Biogeochem. Cycles*, *22*, GB3016, doi:10.1029/2007GB003139.

Meredith, M. P., and J. C. King (2005), Rapid climate change in the ocean west of the Antarctic Peninsula during the second half of the 20th century, *Geophys. Res. Lett.*, *32*, L19604, doi:10.1029/2005GL024042.

Meredith, M. P., M. I. Wallace, S. E. Stammerjohn, I. A. Renfrew, A. Clarke, H. J. Venables, D. R. Shoosmith, T. Souster, and M. J. Leng (2010), Changes in the freshwater composition of the upper ocean west of the Antarctic Peninsula during the first decade of the 21st century, *Prog. Oceanogr.*, *87*(1–4), 127–143, doi:10.1016/j.pocean.2010.09.019.

Meredith, M. P., L. Jullion, P. J. Brown, A. C. Naveira Garabato, and M. P. Couldrey (2014), Dense waters of the Weddell and Scotia Seas: Recent changes in properties and circulation, *Philos. Trans. R. Soc. London, Ser. A*, *372*, 20130041, doi:10.1098/rsta.2013.0041.

Miller, L. A., T. N. Papakyriakou, R. E. Collins, J. W. Deming, J. K. Ehn, R. W. Macdonald, A. Mucci, O. Owens, M. Raudsepp, and N. Sutherland (2011), Carbon dynamics in sea ice: A winter flux time series, *J. Geophys. Res.*, *116*, C02028, doi:10.1029/2009JC006058.

Millero, F. J. (2007), The marine inorganic carbon cycle, *Chem. Rev.*, *107*(2), 308–341, doi:10.1021/cr0503557.

Mintrop, L., F. F. Pérez, M. González, D. J. Magdalena, and C. A. Körtzinger (2000), Alkalinity determination by potentiometry: Intercalibration using three different methods, *Cienc. Mar.*, *26*(1), 23–27.

Mucci, A., B. Lansard, L. A. Miller, and T. N. Papakyriakou (2010), CO_2 fluxes across the air-sea interface in the southeastern Beaufort Sea: Ice-free period, *J. Geophys. Res.*, *115*, C04003, doi:10.1029/2009JC005330.

Nomura, D., M. A. Granskog, P. Assmy, D. Simizu, and G. Hashida (2013), Arctic and Antarctic sea ice acts as a sink for atmospheric CO_2 during periods of snowmelt and surface flooding, *J. Geophys. Res. Oceans*, *118*, 6511–6524, doi:10.1002/2013JC009048.

Papadimitriou, S., H. Kennedy, G. Kattner, G. Dieckmann, and D. Thomas (2004), Experimental evidence for carbonate precipitation and CO_2 degassing during sea ice formation, *Geochim. Cosmochim. Acta*, *68*(8), 1749–1761, doi:10.1016/j.gca.2003.07.004.

Purkey, S. G., and G. C. Johnson (2012), Global contraction of Antarctic bottom water between the 1980s and 2000s, *J. Clim.*, *25*, 5830–5844, doi:10.1175/JCLI-D-11-00612.1.

Roden, N. P., E. H. Shadwick, B. Tilbrook, and T. W. Trull (2013), Annual cycle of carbonate chemistry and decadal change in coastal Prydz Bay, East Antarctica, *Mar. Chem.*, *155*, 135–147, doi:10.1016/j.marchem.2013.06.006.

Rysgaard, S., R. N. Glud, K. Lennert, M. Cooper, N. Halden, R. J. G. Leakey, F. C. Hawthorne, and D. Barber (2012), Ikaite crystals in melting sea ice implications for pCO_2 and pH levels in Arctic surface waters, *Cryosphere*, *6*(4), 901–908, doi:10.5194/tc-6-901-2012.

Rysgaard, S. R., J. R. Bendtsen, B. Delille, G. S. Dieckmann, R. N. Glud, H. Kennedy, J. Mortensen, S. Papadimitriou, D. N. Thomas, and J.-L. Tison (2011), Sea ice contribution to the air-sea CO_2 exchange in the Arctic and Southern Oceans, *Tellus, Ser. B*, *63*(5), 823–830, doi:10.1111/j.1600-0889.2011.00571.x.

Semiletov, I., A. Makshtas, S. -I. Akasofu, and E. L. Andreas (2004), Atmospheric CO_2 balance: The role of Arctic sea ice, *Geophys. Res. Lett.*, *31*, L05121, doi:10.1029/2003GL017996.

Stammerjohn, S. E., D. G. Martinson, R. C. Smith, X. Yuan, and D. Rind (2008), Trends in Antarctic annual sea ice retreat and advance and their relation to El Niño Southern Oscillation and Southern Annular Mode variability, *J. Geophys. Res.*, *113*, C03S90, doi:10.1029/2007JC004269.

Stephens, B. B., and R. F. Keeling (2000), The influence of Antarctic sea ice on glacial-interglacial CO_2 variations, *Nature*, *404*, 171–174.

Sweeney, C. (2003), The annual cycle of surface water CO_2 and O_2 in the Ross Sea: A model for gas exchange on the continental shelves of Antarctica, *Antarct. Res. Ser.*, *78*, 295–312.

Takahashi, T., et al. (2009), Climatological mean and decadal change in surface ocean pCO_2, and net sea air CO_2 flux over the global oceans, *Deep Sea Res., Part II*, *56*, 554–577, doi:10.1016/j.dsr2.2008.12.009.

Thompson, D. W. J., and S. Solomon (2002), Interpretation of recent Southern Hemisphere climate change, *Science*, *296*, 895–899.

Van Heuven, S., D. Pierrot, J. Rae, E. Lewis, and D. Wallace (2011), MATLAB Program developed for CO_2 system calculations, ORNL/CDIAC-105b, Carbon Dioxide Inf. Anal. Cent., Oak Ridge Natl. Lab., U.S. Dep. of Energy, Oak Ridge, Tenn., doi:10.3334/CDIAC/otg.CO2SYS.

Vaughan, D., G. J. Marshall, W. Connelley, C. Parkinson, R. Mulvaney, D. A. Hodgson, J. C. King, C. J. Pudsey, and J. Turner (2003), Recent rapid regional climate warming on the Antarctic Peninsula, *Clim. Change*, *60*, 243–274.

Venables, H. J., and M. P. Meredith (2014), Feedbacks between ice cover, ocean stratification, and heat content in Ryder Bay, western Antarctic Peninsula, *J. Geophys. Res. Oceans*, *119*, 5323–5336, doi:10.1002/2013JC009669.

Venables, H. J., A. Clarke, and M. P. Meredith (2013), Wintertime controls on summer stratification and productivity at the western Antarctic Peninsula, *Limnol. Oceanogr.*, *58*(3), 1035–1047, doi:10.4319/lo.2013.58.3.1035.

Wallace, M. I. (2007), Ocean circulation in Marguerite Bay, PhD thesis, The Open Univ., Milton Keynes, U. K.

Wanninkhof, R. (1992), Relationship between wind speed and gas exchange over the ocean, *J. Geophys. Res.*, *97*(C5), 7373–7382, doi:10.1029/92JC00188.

Wanninkhof, R. (2014), Relationship between wind speed and gas exchange over the ocean revisited, *Limnol. Oceanogr.*, *12*, 351–362, doi:10.4319/lom.2014.12.351.

Wanninkhof, R., et al. (2013), Global ocean carbon uptake: Magnitude, variability and trends, *Biogeosciences*, *10*(3), 1983–2000, doi:10.5194/bg-10-1983-2013.

Weiss, R., and B. Price (1980), Nitrous oxide solubility in water and seawater, *Mar. Chem.*, *8*(4), 347–359, doi:10.1016/0304-4203(80)90024-9.

Weiss, R. F. (1974), Carbon dioxide in water and seawater: The solubility of a non-ideal gas, *Mar. Chem.*, *2*, 203–215.

Zemmelink, H. J., B. Delille, J. L. Tison, E. J. Hintsa, L. Houghton, and J. W. H. Dacey (2006), CO_2 deposition over the multi-year ice of the western Weddell Sea, *Geophys. Res. Lett.*, *33*, L13606, doi:10.1029/2006GL026320.